

NASA Contractor Report 198327

ICASE Report No. 96-27

ICASE

NONLINEAR EXCITATION OF INVISCID STATIONARY VORTEX IN A BOUNDARY-LAYER FLOW

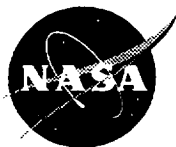
Meelan Choudhari

Peter W. Duck

*NASA Contract No. NAS1-19480
April 1996*

*Institute for Computer Applications in Science and Engineering
NASA Langley Research Center
Hampton, VA 23681-0001*

Operated by Universities Space Research Association



*National Aeronautics and
Space Administration*

*Langley Research Center
Hampton, Virginia 23681-0001*

Nonlinear Excitation of Inviscid Stationary Vortex in a Boundary-Layer Flow

Meelan Choudhari¹

High Technology Corporation
Hampton, VA 23666, USA

Peter W. Duck²

University of Manchester
Manchester, M13 9PL, UK

Abstract

We examine the excitation of inviscid stationary crossflow instabilities near an isolated surface hump (or indentation) underneath a three-dimensional boundary layer. As the hump height (or indentation depth) is increased from zero, the receptivity process becomes nonlinear even before the stability characteristics of the boundary layer are modified to a significant extent. This behavior contrasts sharply with earlier findings on the excitation of the lower branch Tollmien-Schlichting modes and is attributed to the inviscid nature of the crossflow modes, which leads to a decoupling between the regions of receptivity and stability. As a result of this decoupling, similarity transformations exist that allow the nonlinear receptivity of a general three-dimensional boundary layer to be studied with a set of canonical solutions to the viscous sublayer equations. The parametric study suggests that the receptivity is likely to become nonlinear even before the hump height becomes large enough for flow reversal to occur in the canonical solution. We also find that the receptivity to surface humps increases more rapidly as the hump height increases than is predicted by linear theory. On the other hand, receptivity near surface indentations is generally smaller in comparison with the linear approximation. Extension of the work to crossflow receptivity in compressible boundary layers and to Görtler vortex excitation is also discussed.

¹The work of MC was supported by NASA Langley Research Center under contract number NAS1-20059.

²The research of the second author was supported by the National Aeronautics and Space Administration under NASA Contract No. NAS1-19480 while he was in residence at the Institute for Computer Applications in Science and Engineering (ICASE), NASA Langley Research Center, Hampton, VA 23681-0001.

1 Introduction

Our concern in this paper is with the excitation of stationary vortex instabilities in a boundary-layer flow. Our main focus is on the excitation of stationary crossflow (i.e., Rayleigh) modes of an incompressible three-dimensional boundary layer; the excitation is caused by isolated roughness elements (e.g., humps or indentations) on an otherwise smooth surface. However, some consideration is also devoted to the effects of compressibility and to the excitation of Görtler vortex instabilities.

The above problems fall under the category of boundary-layer receptivity (Morkovin, 1969), which represents the first stage of the laminar to turbulent transition process in the boundary layer. Receptivity problems have received increasing attention in recent years, mainly as a consequence of theoretical breakthroughs made by Goldstein (1983, 1985), Zavol'skii, Reutov, and Ryboushkina (1983), and Ruban (1985) on generation of Tollmien-Schlichting (TS) modes of instability by unsteady free-stream disturbances. In producing the TS waves the free-stream disturbances may act alone, or in conjunction with stationary surface irregularities such as surface humps.

The excitation of stationary crossflow modes by small-amplitude surface disturbances was first investigated by Wilkinson and Malik (1985) as part of their pioneering experiments on the rotating disk boundary layer. More recently, receptivity on swept-wing models was examined in wind-tunnel experiments by Dovgal et al. (1989); Kachanov and Tararykin (1990); and Radeztsky et al. (1991). Theoretical predictions for the crossflow receptivity have been developed by Fedorov (1988); Manuilovich (1990); Choudhari and Streett (1990); Choudhari (1993); and Crouch (1993). All of these analyses used suitable extensions of the linearized version of the Goldstein (1985)-Ruban (1985) theory, so that the amplitude of the generated instability motion scaled linearly with respect to the height of the surface irregularity.

In the present work, we examine the receptivity to moderately strong (short-scale) perturbations in the surface height, such that local flow reversal may occur and such that the linear relationship between the input and the output of the receptivity process is no longer valid. Analogous calculations in the context of (two-dimensional) TS wave generation have been presented earlier by Bodonyi, Tadjfar, Duck, and Welch (1989); and Nayfeh and Ashour (1994). Their work indicated that the amplitude of the TS wave increases with hump height

at a faster than linear rate.

The main feature of stationary receptivity problems that involves surface irregularities is that a stationary irregularity can directly excite the instability modes of interest (i.e., without any interaction with the free-stream unsteadiness, which is the case with TS-wave excitation). Moreover, Goldstein (1985) and Ruban (1985) have shown that the surface irregularities that are strong enough to provoke a nonlinear receptivity mechanism in the TS case also can alter the stability properties of the underlying base flow to leading order. In contrast, we demonstrate that for a large class of stationary vortex instabilities, the receptivity becomes a nonlinear function of the amplitude of the surface irregularity before the irregularity can exert a significant influence on the stability properties of the vortex mode of interest. This simplification arises from the fact that the receptivity occurs in a thin sublayer close to the surface (where the nonlinear response to the irregularity is concentrated), whereas the vortex instabilities that are predominantly inviscid are controlled by the main boundary-layer region (where the disturbance produced by the surface irregularity is weak).

This paper is organized as follows. In section 2, we formulate the problem and present a brief description of the receptivity analysis. This section shows that for surface irregularities with a circular planform the problem of the excitation of stationary inviscid crossflow instabilities in a general class of boundary layers can be studied with a set of canonical solutions to the viscous-sublayer equations; these equations were originally derived by Smith (1976) in the context of the interaction of the hump with a two-dimensional boundary layer. A description of the numerically obtained canonical solutions for a representative hump geometry is given in section 3. Those solutions are also applied in the prediction of receptivity in section 3. Finally, some conclusions are drawn in section 4.

In this paper, we assume that the three-dimensional boundary layer is convectively unstable (Huerre and Monkewitz, 1990) within the region of the receptivity, so that the large-time response of the flow to the surface irregularity can be studied with time independent equations. According to some recent evidence (Lingwood, 1995), the crossflow modes lead to an absolute instability in at least one case of three-dimensional boundary layers when the Reynolds number parameter becomes sufficiently large. However, there is compelling experimental evidence (Riebert et al., 1996) that the conditions required for absolute instability may not always be met in practice and that transition in certain flows of technological interest is attributed to spatially amplifying crossflow instabilities. The neglect of unsteady

effects associated with any vortex shedding from the irregularity is also supported by the experimental observations of Kachanov and Tararykin (1990).

2 Analysis

Consider a three-dimensional incompressible boundary layer that encounters a three-dimensional surface hump (or indentation) on an otherwise smooth underlying surface. The edge velocity Q^* and the thickness L^* of the boundary layer just upstream of this hump are taken to be the reference velocity and the reference length scale, respectively. For the disturbance produced by the hump to couple with the inviscid crossflow modes of the incoming boundary layer, we assume that the planform dimensions of the hump are both $O(1)$ quantities.

It may be inferred from the analysis of Smith (1976) that when the hump height is sufficiently small in comparison with $R^{-1/3}$ (where $R \gg 1$ is the reference Reynolds number) the steady disturbance produced by the hump is a linear perturbation to the incoming boundary layer. Moreover, the disturbance structure is split into two distinct subregions along the direction y that is normal to the unperturbed surface. The disturbance has its largest amplitude within a thin layer (with a thickness of $O(R^{-1/3})$) next to the surface, where it is strongly influenced by the viscous diffusion of vorticity away from the surface. The outer subregion corresponds to the main part of the incoming boundary layer (i.e., $y = O(1)$), where the disturbance is weaker and is predominantly inviscid.

The most noteworthy characteristic of the above disturbance field is that the viscous sublayer completely absorbs the vertical displacement produced by the hump, thereby leaving the outer layers of fluid relatively undisplaced. As a result of this cushioning effect provided by the sublayer, this flow regime has been known as the “compensation regime” in Russian literature (Bogolepov, 1985). In other words, the viscous action within the sublayer converts the displacement of the flow (by the hump) into a normal velocity flux that drives the motion within the outer region and during that process excites the eigenmodes of the outer flow, which are precisely the inviscid vortex instabilities of interest (Choudhari, 1993).

As the hump height is gradually increased so as to become comparable with the thickness of the viscous sublayer, the flow response becomes nonlinear in that region. To calculate this response, we introduce the Prandtl-transposed coordinate $Y = R^{1/3}y - hF(x, z)$, where $h (= O(1))$ and $F(x, z)$ represent the amplitude and the shape, respectively, of the height

distribution associated with the surface irregularity; x and z denote a suitably chosen pair of orthogonal coordinate axes along the surface. The velocity components along the x, y , and z directions and the (incremental) pressure within the sublayer region $Y = O(1)$ can then be expanded in the form

$$(u, v, w, p) = \epsilon [U, \epsilon(V + hF_x U + hF_z W), W, \epsilon P] + \dots, \quad (1)$$

where $\epsilon \equiv R^{-1/3}$; the subscripts x and z indicate partial differentiation with respect to the indicated coordinate. The leading-order quantities in (1) are governed by the three-dimensional boundary-layer equations

$$U_x + V_Y + W_z = 0, \quad (2a)$$

$$UU_x + VU_Y + WU_z = -P_x + U_{YY}, \quad (2b)$$

$$P_Y = 0, \quad (2c)$$

$$UW_x + VW_Y + WW_z = -P_z + W_{YY} \quad (2d)$$

that are subject to the boundary conditions

$$U = V = W = 0 \quad \text{at} \quad Y = 0, \quad (3a, b, c)$$

$$U \sim \lambda_1(Y + hF) + O(1/Y), \quad W \sim \lambda_3(Y + hF) + O(1/Y), \quad (3d, e)$$

and

$$U \sim \lambda_1 Y, \quad V \rightarrow 0, \quad W \sim \lambda_3 Y \quad \text{as} \quad x^2 + z^2 \rightarrow \infty \quad \text{at each } Y, \quad (3f, g, h)$$

Here $\lambda_1 \equiv dU_b(y=0)/dy$ and $\lambda_3 \equiv dW_b(y=0)/dy$ are the slopes at the wall of the velocity profiles of the boundary-layer flow as it approaches the hump.

The ‘‘compensation’’ conditions (3d) and (3e), together with (2a), show that

$$V + hF_x U + hF_z W \rightarrow \mathcal{C}(x, z) \quad \text{as} \quad Y \rightarrow \infty, \quad (4)$$

where the sublayer flux $\mathcal{C}(x, z)$ is determined as part of the output from the viscous-sublayer problem. The perturbations in the main boundary-layer region ($y = O(1)$) that are driven by this sublayer flux can be expanded in the form

$$(u, v, w, p) = [U_b(y), 0, W_b(y), 0] + \epsilon^2(u_1, v_1, w_1, p_1) + \dots, \quad (5)$$

where u, v, w , and p are now functions of x, y , and z . To analyze the receptivity problem, we can easily solve for (u_1, v_1, w_1, p_1) by using the Fourier transformation $x \rightarrow \alpha$ and $z \rightarrow \beta$. The Fourier transform \bar{v}_1 of the normal velocity perturbation satisfies the stationary form of Rayleigh's equation

$$\{(\alpha U_0 + \beta W_0)[d^2/dy^2 - (\alpha^2 + \beta^2)] - (\alpha U_0'' + \beta W_0'')\} \bar{v}_1(y; \alpha, \beta) = 0, \quad (6a)$$

which governs the crossflow instability in a three-dimensional boundary layer; see Gregory, Stuart, and Walker (1955) and Hall (1986). The requirement of asymptotic matching with the sublayer solution imposes the inhomogeneous boundary condition at the surface

$$\bar{v}_1 = \bar{C}(\alpha, \beta) \text{ at } y = 0. \quad (6b)$$

With the assumption that the boundary-layer flow is convectively unstable locally, the crossflow instabilities arise as part of the causal solution to the inhomogeneous stationary Rayleigh problem. In particular, the part of the total normal velocity perturbation v_1 that corresponds to the unstable mode of crossflow instability is given by

$$v_{cf}(x, y, z) = \frac{1}{\sqrt{2\pi}} \int_{\Gamma_\beta} \hat{v}_{cf}(\beta) E_{cf}(y, \beta) e^{h(\beta; z/x)x} d\beta \quad (7a)$$

where $h(\beta) = i[\alpha_{cf}(\beta) + (z/x)\beta]$. In deriving (7a), we have chosen to invert the transform in x first; Γ_β denotes the inversion contour in the β plane; $\alpha_{cf}(\beta)$ and $E_{cf}(y, \beta)$ denote the eigenvalue and the (appropriately normalized) eigenfunction, respectively, for the unstable crossflow mode with wave number β in the z direction; and \hat{v}_{cf} is the initial amplitude spectrum of the generated crossflow modes. Because of the linear character of (6a) and (6b), \hat{v}_{cf} can be expressed as the product

$$\hat{v}_{cf}(\beta) = \bar{C}[\alpha_{cf}(\beta), \beta] \Lambda(\beta) \quad (7b)$$

where the function $\Lambda(\beta)$ is independent of the hump geometry (i.e., it is solely determined by the upstream boundary-layer profiles and the wave number of the crossflow mode of interest). (See Goldstein (1985).) The form of (7b) is similar to equation (2.7b) of Choudhari and Streett (1990), who studied the same problem in the context of a rotating-disk boundary layer for sufficiently small values of the height parameter h . We also note that, because of the broad spatial spectrum of the induced disturbance motion, critical-layer effects do not become important within the local region of receptivity.

For $h \ll 1$, the sublayer outflux is given by the analytical expression

$$\bar{\mathcal{C}}(\alpha, \beta) = -3Ai'(0)[i(\alpha\lambda_1 + \beta\lambda_3)]^{2/3}h\bar{F}, \quad (7c)$$

where Ai' denotes the derivative of the Airy function of the first kind. Thus, in the linear case, the amplitude of any crossflow mode that is generated locally can be directly related to the amplitude of the resonant Fourier harmonic of the surface height distribution. For $h = O(1)$, the effects of the height and the shape of the hump cannot be separated in this simple manner, and the dependence of the spectral-density function on the hump geometry becomes quite nontrivial.

The far downstream evolution of the instability motion can be easily determined by the steepest descent approximation to the integral in (7a). The contribution to this integral from each relevant saddle point $\beta^\#$ of $h(\beta)$ is given by

$$v_{cf}(x, y, z) \sim \sqrt{\frac{2\pi}{-h''(\beta^\#)x}} \hat{v}_{cf}(\beta^\#) e^{h(\beta^\#)x} \quad (8)$$

as $x \rightarrow +\infty$ over the local length scale. saddle point of $h(\beta)$ in the If more than one saddle point is relevant, then a summation must be taken; however, in the far downstream limit only the saddle point(s) with the largest exponential growth rate are expected to make the dominant contribution to the right-hand side of (7a).

The vertical outflux function $\mathcal{C}(x, z)$ exhibits a similar behavior:

$$\mathcal{C}[x, z; \lambda_1, \lambda_3, h, F(x, z)] = \frac{1}{a} \mathcal{C}[\hat{x}, \hat{z}; 1, 0, \hat{h}, \hat{F}(\hat{x}, \hat{z})] \quad (9a)$$

where the canonical coordinates $(\hat{x}, \hat{z}) = 1/(\lambda a^3)(\cos \theta_w x + \sin \theta_w z, -\sin \theta_w x + \cos \theta_w z)$ are defined such that the \hat{x} axis is aligned with the wall-shear vector $(\lambda_1, \lambda_3) = \lambda(\cos \theta_w, \sin \theta_w)$. Moreover, $\hat{h} = h/a$ and $\hat{F}(\hat{x}, \hat{z}) = F(x, z)$. The stretching parameter a can be chosen arbitrarily and has been set equal to $\lambda^{-2/3}$ in this paper, so that the value of the scaled height parameter \hat{h} does not depend on the choice of the reference length scale (i.e., the particular chosen measure for the thickness of the upstream boundary layer). When the hump geometry function $F(x, z)$ has an azimuthal symmetry (i.e., F depends on x and z only through $r = \sqrt{x^2 + z^2}$), then $\hat{F}(\hat{x}, \hat{z}) = F[\hat{x}/(\lambda a^3), \hat{z}/(\lambda a^3)]$. Thus,

$$\mathcal{C}[x, z; \lambda_1, \lambda_3, h, F(x, z)] = \frac{1}{a} \mathcal{C}[\hat{x}, \hat{z}; 1, 0, \hat{h}, F(\hat{x}/(\lambda a^3), \hat{z}/(\lambda a^3))] \quad (9b)$$

Equation (9b) represents a powerful simplification; the receptivity of a general three-dimensional boundary layer to surface irregularities that correspond to a given family of azimuthally symmetric shape functions can now be studied with a set of canonical solutions to the viscous sublayer problem in the (\hat{x}, Y, \hat{z}) coordinates.

3 Results

3.1 Numerical Solution to the Viscous Sublayer Problem

The canonical sublayer problem (i.e., with $\lambda_1 = 1$, $\lambda_3 = 0$) was solved numerically for $\hat{F}(\hat{x}, \hat{z}) = \exp[-(\hat{x}^2 + \hat{z}^2)/\hat{r}_0]$ with $\hat{r}_0 = 2$. A slightly modified version of the numerical scheme proposed by Smith (1991) was used; the latter scheme combines multiple forward-marching sweeps in constant- \hat{z} planes with a Poisson solver for the pressure distribution to account for the upstream influence in the problem. A second-order-accurate discretization was used along each spatial coordinate for both the forward marching sweep and the Poisson equation. The Poisson equation was solved by imposing a Dirichlet boundary condition at the upstream end of the computational domain and either a Neumann or a Dirichlet condition at the outflow boundary. The choice of Neumann boundary condition usually led to a better overall solution, especially in terms of the velocity distribution in the region downstream of the hump; however, the Dirichlet condition yielded more satisfactory behavior (i.e., decay) of the pressure perturbations in that region. Despite these differences, we found that the sublayer outflux \mathcal{C} (the only quantity of interest from the standpoint of receptivity) was nearly insensitive to the type of boundary condition imposed, so that the outflux distributions for different treatments at the downstream boundary were graphically indistinguishable. This agreement boosted our confidence in regard to the adequacy of the computed solution.

Figures 1(a) and 1(b) show the variation in the outflux distribution along the \hat{x} axis with an increase in the magnitude of the height parameter \hat{h} across the ranges of $\hat{h} > 0$ (i.e., a hump) and $\hat{h} < 0$ (i.e., an indentation), respectively. At the extreme values of \hat{h} , namely, $\hat{h} = +4$ and $\hat{h} = -3$, a small region of axial flow reversal exists over the leeward and windward sections, respectively, of the hump. The ordinate in each of these plots has been scaled by the respective value of \hat{h} , and for comparison we have also indicated the linearized solution (7c) by means of a dashed curve. (Note that in the linear case the outflux variation along the \hat{z} direction is exactly the same as that of the geometry function $F(\hat{x}, \hat{z})$.) As one

might intuitively expect, in the case of surface humps the outflow in the region upstream of the hump center ($\hat{x} = 0$) is accompanied by an inflow in the leeward region. For indentations, an inflow is present upstream; an outflow exists in the leeward region.

It is easily shown that the inward and outward fluxes must balance each other, so that the net outflux (i.e., $\int_{-\infty}^{\infty} \mathcal{C}(\hat{x}, \hat{z}) d\hat{x}$) is equal to zero. The zero net flux is the consequence of a conservation law that is based on the \hat{x} -momentum equation (2b) and the requirement that the hump-induced disturbances must decay both upstream and downstream of the hump (i.e., equations (3f) through (3h)). One can similarly show that the x -averaged wall-shear perturbation is also equal to zero. The two conservation integrals can be used, in principle, to check the accuracy of the numerical scheme. However, because the hump-induced perturbations decay rather slowly in the x direction and because we did not employ any grid stretching along that direction (which necessarily limited the grid extent), we were not able to validate the numerical results using the above two tests.

For $\hat{h} = +1$, the effect of nonlinearity on the outflux distribution is small, so that its axial variation is graphically identical to the linear prediction based on (7c). Nonlinear effects appear as the hump height is increased beyond unity. In particular, nonlinearity enhances the levels of both the upstream outflow and the downstream inflow; however, the qualitative nature of the axial outflux distribution remains roughly similar to the linear result, except for a stronger increase in the peak outflow and an upstream shift in the location of the peak inflow. The above similarity suggests that the shape of the Fourier spectrum, too, will be correspondingly similar to that based on the linear prediction in the range of $O(1)$ wave numbers but that the amplitude levels will increase at a faster than linear rate as the hump height is increased. This expectation is corroborated by the numerical findings, which are described in section 3.2.

3.2 Receptivity Prediction

Although the analysis in section 2 is applicable to a general class of three-dimensional boundary layers, we restrict ourselves to the Falkner-Skan-Cooke (FSC) family of self-similar boundary layers for the purpose of a parametric study. The boundary-layer profiles from the FSC family are distinguished on the basis of the Hartree parameter H and the local sweep angle θ_e (which is measured with respect to the x direction). We choose the reference length scale for these boundary layers to be $L^* = \{Q^* \cos \theta_e / [(2 - H) \nu^* \ell^*]\}^{-1/2}$, where ℓ^* denotes

the distance between the leading edge and the surface irregularity and ν^* is the kinematic viscosity of the fluid. A detailed stability investigation for the FSC boundary layers was carried out by Mack (1984).

As shown by (8), the instability motion along each direction $\theta = \arctan(z/x)$ is dominated by a narrow group of wave-number vectors that is centered on that crossflow mode(s) which corresponds to the dominant saddle point(s) for that particular direction. Therefore, in order to characterize the effect of nonlinearity on the locally generated instability motion, we can examine how the Fourier amplitude of the outflux distribution at the saddle-point location (i.e., $\bar{\mathcal{C}}[\alpha_{cf}(\beta^\#), \beta^\#]$) varies as \hat{h} is varied. Because the dominant saddle point $\beta^\#$ can only be determined after considering the global topology (in the complex β plane) of the integrand in (7a), we carried out a global numerical search for the saddle points of $h(\beta)$ in one specific case, namely, that with $H = 0.6$ and $\theta_e = \pi/4$. (Mack (1984) shows that the latter value of sweep angle yields the largest crossflow velocity at any given H .) In order to carry out this search, the $h(\beta)$ function was analytically continued from its values along the real β axis. Because of the symmetry of the dispersion function $\alpha_{cf}(\beta)$ (namely, $\alpha_{cf}(\beta^*) = -\alpha_{cf}^*(\beta)$, where the asterisk denotes the complex conjugate), the search for saddle points was confined to the right half of the β plane.

The above search revealed only one family (or trajectory) of saddle points (which is parameterized by θ) inside a rectangular region with vertices at the wave-number locations $(0, \pm 0.5)$ and $(1.5, \pm 0.5)$ in the complex β plane. This trajectory crosses the real β axis at the location $\beta_{mg}^\#$, which corresponds to the vortex mode that has the maximum spatial growth rate $-\text{Im}(\alpha_{cf}(\beta))$ for any real β , as well as the maximum growth rate $\text{Re}(h(\beta^\#))$ for any $\beta^\#$ on the saddle-point trajectory. Note that the existence of other saddle-point trajectories outside the above search region should not be discounted *a priori*. Moreover, we also have not addressed the issue of global contour deformation that would establish the relevance of the above saddle-point trajectory to the integral in (7a). Nevertheless, the findings from the saddle-point search strongly suggest that this trajectory is the only one that is relevant to the unstable crossflow modes. (This behavior is quite different from the lower branch TS modes, for which more than one saddle-point family can be relevant (Choudhari and Kerschen 1990).) Accordingly, the relevant saddle-point trajectory for other FSC boundary layers can be easily determined by marching away from the saddle point $\beta_{mg}^\#$ on the real β axis.

To compute the Fourier transform of the numerically obtained sublayer outflux, we used a spline fit in \hat{x} and \hat{z} to $\mathcal{C}(\hat{x}, \hat{z})$. The contribution to the Fourier transform from each spline interval was evaluated with closed form expressions based on the spline coefficients. The contribution from the tail region that lies beyond the outflow location was also estimated via a first-order algebraic extrapolation from the computed solution. The linear solution for $h \ll 1$ was used as one of the checks on the calculation of the Fourier transform; the computed spectrum was found to be within 0.2 percent of the analytical solution (8).

Figure 2(a) shows the variation in the magnitude of the Fourier transform $\bar{\mathcal{C}}[\alpha_{cf}(\beta_{mg}^\#), \beta_{mg}^\#]$ with the canonical height parameter \hat{h} for $\hat{r}_0 = 2$. In the specific case considered (namely, $H = 0.6$ and $\theta_e = \pi/4$), $\beta_{mg}^\# \approx (0.545, 0)$ and $\alpha_{cf}(\beta_{mg}^\#) \approx (-0.49, -0.027)$. The computed value of $\bar{\mathcal{C}}$ for $\hat{h} = +1$ is very nearly equal to the value computed with linear theory, but a nonlinear increase in $|\bar{\mathcal{C}}|$ is observed for an \hat{h} that is larger than unity. On the other hand, nonlinearity appears to suppress the receptivity that is induced by surface indentations ($\hat{h} < 0$).

The geometry function F for a given family of azimuthally symmetric surface irregularities is parameterized by the height h and the planform radius r_0 . However, the similarity behavior (9b) enables one to span the two-parameter $(h - r_0)$ space with the one-parameter family of canonical solutions, which was obtained by varying \hat{h} at a fixed \hat{r}_0 . Specifically, if the physical roughness dimension r_0 were to be changed, then the stretching parameter a in (9b) could be modified such that the canonical radius \hat{r}_0 remains the same (equal to 2 in the present case). Of course, a different effective height \hat{h} is now obtained; the Fourier transform of the canonical outflux distribution $\mathcal{C}(\hat{x}, \hat{z})$ must be evaluated at a wave-number vector $(\hat{\alpha}, \hat{\beta})$ that has the same orientation as before, with a smaller or larger magnitude depending on whether the planform size increases or decreases, respectively.

Because of the abovementioned simplification, we now examine the Fourier spectrum of $\mathcal{C}(\hat{x}, \hat{z})$ as a function of $(\hat{\alpha}^2 + \hat{\beta}^2)^{1/2}$ for real values of $\hat{\alpha}$ and $\hat{\beta}$. (See fig. 2(b).) The orientation of the wave-number vector is chosen to be the same as that of the most unstable mode $(\alpha_{cf}(\beta_{mg}^\#), \beta_{mg}^\#)$ at $H = 0.6$ and $\theta_e = \pi/4$. Figure 2(b) shows that in a large range of wave-number magnitudes or, alternatively, in a large range of planform sizes the hump-induced receptivity along the direction of maximum growth will increase at a faster than linear rate for $h > 0$ and at a slower rate for $h < 0$. The nonlinear increase in receptivity for $h > 0$ is qualitatively consistent with the experimental measurements of Kachanov and

Tararykin (1990). However, one must also note that the experiments were carried out for roughness elements that had square-shaped planforms (as against the circular planform used in the calculations above) and also had relatively large heights (comparable to the thickness of the boundary layer).

4 Conclusions

The objective of this study was to assess the effect of nonlinearity on the generation of stationary inviscid instabilities by means of an isolated surface irregularity. Because of the decoupling between the regions of receptivity and stability, the receptivity process became nonlinear even before the height perturbations became large enough to significantly modify the stability characteristics of the boundary layer. As a result of the existence of a similarity transform for the sublayer problem, a one-parameter family of canonical solutions was used to study the generation of stationary crossflow vortices in a general three-dimensional boundary layer for a wide range of hump or indentation sizes. The limited parametric study carried out in this paper revealed a nonlinear increase in hump-induced receptivity as the height parameter was increased, but the receptivity attributed to an indentation was smaller in comparison with the prediction based on linear theory. We suspect that the above conclusions may actually be valid in a wide range of cases. However, there is a need to verify the above trends with controlled wind-tunnel experiments and/or direct numerical simulations, especially at the larger height perturbations and at the relatively moderate Reynolds numbers that are encountered in practical situations.

The present analysis can be easily extended to include the receptivity of compressible (subsonic or supersonic) boundary layers. Because the boundary-layer velocities in the sublayer region are asymptotically small, the flow within that region is effectively incompressible even when the local free stream is supersonic. Thus, the analysis in section 2 applies directly to the compressible case, provided that one replaces the incompressible Rayleigh's equation (4) by its compressible counterpart and computes the $\Lambda(\beta)$ function based on the latter equation.

The present analysis also implies that the nonlinear excitation of inviscid Görtler vortex modes (Denier et al., 1990; Timoshin, 1990) can be studied with a set of canonical solutions that do not depend on the form of the upstream boundary-layer profile(s). The Görtler

modes are more efficiently excited by roughness elements that are elongated in the flow direction. For such irregularities, the gradient of the induced pressure along the streamwise direction becomes relatively small. Therefore, the sublayer problem becomes parabolic in that direction, which simplifies the nonlinear receptivity calculation to a considerable extent. Numerical solutions to this simplified problem for representative distributions of surface irregularities are being pursued currently.

5 Acknowledgments

The authors are grateful to Dr. M.E. Goldstein for his encouragement and for his valuable comments during the early stages of this work. A number of computations were performed using facilities provided by EPSRC.

References

- [1] Bodonyi, R. J., Welch, W. J. C., Duck, P. W., and Tadjfar, M., "A Numerical Study of the Interaction Between Unsteady Free-Stream Disturbances and Localized Variations in Surface Geometry," *J. Fluid Mech.*, Vol. 209, pp. 285-308, 1989.
- [2] Bogolepov, V. V., "Investigation of three-dimensional local laminar flows," *Zhurnal Prikladnoi Mekhaniki i Tekhnicheskoi Fiziki*, p, 28-36, Jan.-Feb. 1985.
- [3] Choudhari, M., and Streett, C. L., "Boundary Layer Receptivity Phenomena in Three-Dimensional and High-Speed Boundary Layers," AIAA Paper 90-5258, 1990.
- [4] Choudhari, M., "Roughness-Induced Generation of Crossflow Vortices in Three-Dimensional Boundary Layers," NASA CR-4405, 1993. (*Theor. and Comp. Fluid Dyn.*, Vol. 5, pp. 1-31, Feb. 1994.)
- [5] Choudhari, M., and Kerschen, E. J., "Instability Wave Patterns Generated by Interaction of Sound Waves with Three-Dimensional Wall Suction or Roughness," AIAA Paper No. 90-0119, 1990.
- [6] Crouch, J. F., "Receptivity of Three-Dimensional Boundary Layers," AIAA Paper 93-0074, 1993.

- [7] Denier, J. P., Hall, P., and Seddougui, S. O., "On the Receptivity Problem for Görtler Vortices: Vortex Motions Induced by Wall Roughness," ICASE Report 90-31, 1990. (*Phil. Trans. R. Soc. Lond. A.*, Vol. 335, pp. 51-85, 1991).
- [8] Dov'gal, A. V., Kozlov, V. V., and Simonov, O. A., "Sonic Excitation of the Oscillations of the Boundary Layer on a Yawing Wing," *Scientific Proc. TsAGI*, Vol. XX, No. 6, pp. 48-61, 1989.
- [9] Fedorov, A. V., "Excitation of secondary flow instability waves in a boundary layer on a yawed wing," *Zhurnal Prikladnoi Mekhaniki i Tekhnicheskoi Fiziki*, p. 46-52, Sept.-Oct. 1988.
- [10] Goldstein, M. E., "The Evolution of Tollmien-Schlichting Waves Near a Leading Edge," *J. Fluid Mech.*, Vol. 127, pp. 59-81, 1983.
- [11] Goldstein, M. E., "Scattering of Acoustic Waves into Tollmien-Schlichting Waves by Small Streamwise Variations in Surface Geometry," *J. Fluid Mech.*, Vol. 154, pp. 509-529, 1985.
- [12] Gregory, N., Stuart, J. T., and Walker, W. S. "On the Stability of Three Dimensional Boundary Layers with Application to the Flow due to a Rotating Disk," *Phil. Trans. R. Soc. Lond. A*, Vol. 248, pp. 155-199, 1955.
- [13] Hall, P., "An Asymptotic Investigation of the Stationary Modes of Instability of the Boundary Layer on a Rotating Disk," *Proc. Roy. Soc. Lond. A*, Vol. 406, p. 93, 1986.
- [14] Kachanov, Y. S., and Tararykin, O. I., "The Experimental Investigation of Stability and Receptivity of a Swept-Wing Flow," in *Proc. IUTAM Symp. on Laminar Turbulent Transition*, D. Arnal, and R. Michel (Eds.), Springer-Verlag Berlin Heidelberg, 1990.
- [15] Mack, L.M., "Boundary Layer Linear Stability Theory," in AGARD Report 709, 1984.
- [16] Manuilovich, S. V., "Disturbances of a Three-Dimensional Boundary Layer Generated by Surface Roughness," *Fluid Dynamics*, pp. 764-769, Mar. 1990.

- [17] Morkovin, M. V., "Critical Evaluation of Transition from Laminar to Turbulent Shear Layers with Emphasis on Hypersonically Traveling Bodies," AFFDL-TR-68-149, Air Force Flight Dynamics Laboratory, Wright Patterson Air Force Base, Dayton, Ohio, 1969.
- [18] Nayfeh, A. H., and Ashour, O. N., "Acoustic Receptivity of a Boundary Layer to Tollmien-Schlichting Waves Resulting from a Finite-Height Hump at Finite Reynolds Numbers," *Phys. Fluids*, Nov. 1994.
- [19] Radeztsky, R. H., Jr., Reibert, M. S., Saric, W. S., and Takagi, S., "Role of Micron-Sized Roughness in Transition of Swept-Wing Flows," *Bull. Amer. Phys. Soc.*, Vol. 36, No. 10, p. 2630, 1991.
- [20] Ruban, A. I., "On the Generation of Tollmien-Schlichting Waves by Sound," Transl. in *Fluid Dyn.*, Vol. 19, pp. 709-16, 1985.
- [21] Smith, F. T., "Steady and Unsteady 3-D Interactive Boundary Layers," *Computers and Fluids*, pp. 243-268, 1991.
- [22] Smith, F. T., "Pipeflows Distorted by Nonsymmetric Indentation or Branching," *Mathematika*, Vol. 23, pp. 62-83, 1976.
- [23] P. Huerre, and P. A. Monkewitz, "Local and Global Instabilities in Spatially Developing Flows," *Ann. Rev. Fluid Mech.*, Vol. 22, pp. 473-537, 1990.
- [24] Lingwood, R. J., "Absolute Instability of the Boundary Layer on a Rotating Disk," *J. Fluid Mech.*, Vol. 299, pp. 17-33, 1995.
- [25] Timoshin, S. N., "Asymptotic Analysis of a Spatially Unstable Görtler Vortex Spectrum," *Mekh. Zidk. Gaza*, No. 1, 32-41, 1990.
- [26] Wilkinson, S. P., and Malik, M. R., "Stability Experiments in the Flow over a Rotating Disk," *AIAA J.*, Vol. 23 (4), p. 558, 1985.
- [27] Zaval'skii, N. A., Reutov, V. P., and Ryboushkina, G. V., "Generation of Tollmien-Schlichting Waves via Scattering of Acoustic and Vortex Perturbations in Boundary Layer on Wavy Surface," *J. Appl. Mech. Techn. Physics*, pp. 79-86, 1983.

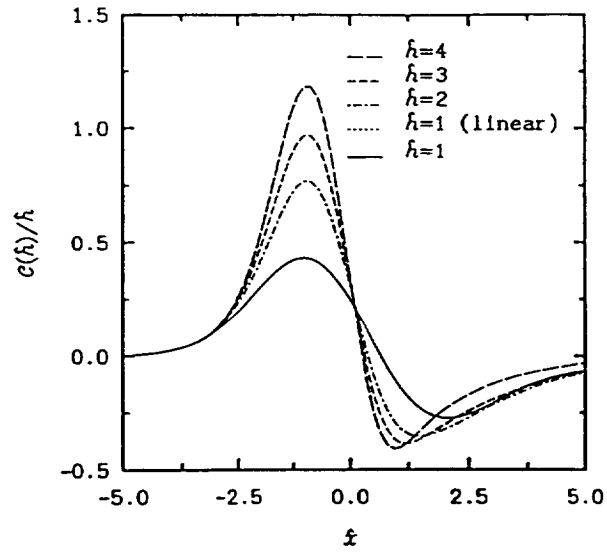


Figure 1a: Axial variation of outflux distribution for various hump heights.

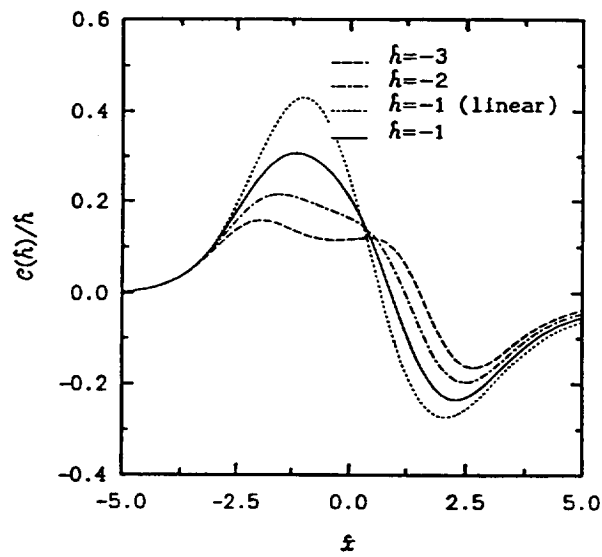


Figure 1b: Axial variation of outflux distribution for various indentation depths.

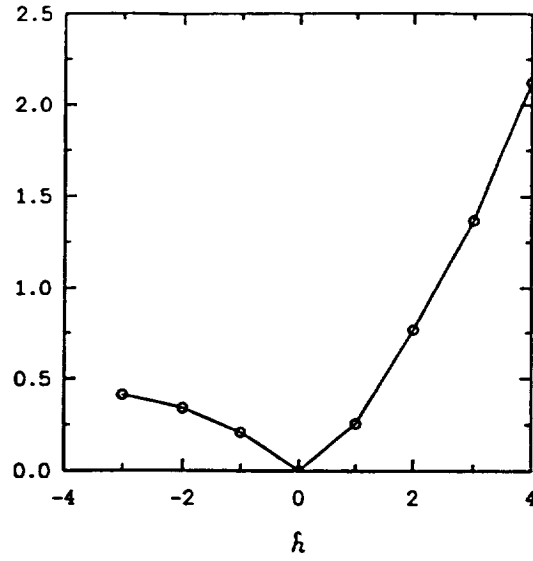


Figure 2a: Effect of nonlinear height perturbations on initial amplitude of most unstable mode at $H = 0.6, \theta_e = \pi/4$. (Scale on ordinate is arbitrary.)

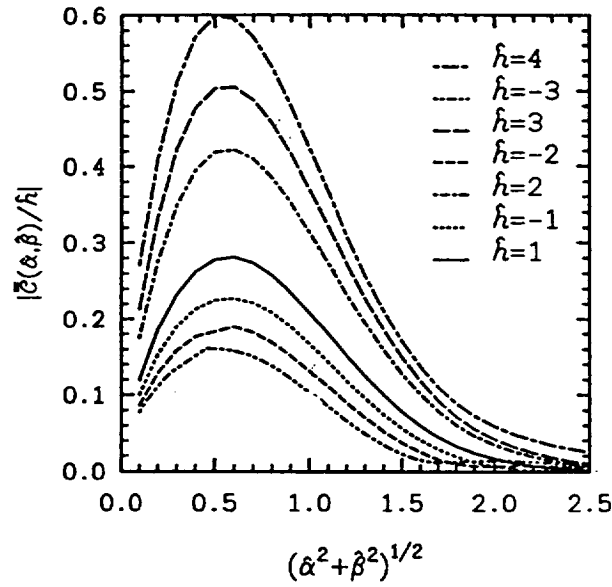


Figure 2b: Fourier spectrum of $\mathcal{C}(\hat{\alpha}, \hat{\beta})$ for various height perturbations. Orientation of wave number vector corresponds to that of most unstable mode at $H = 0.6, \theta_e = \pi/4$.

REPORT DOCUMENTATION PAGE

Form Approved
OMB No. 0704-0188

Public reporting burden for this collection of information is estimated to average 1 hour per response, including the time for reviewing instructions, searching existing data sources, gathering and maintaining the data needed, and completing and reviewing the collection of information. Send comments regarding this burden estimate or any other aspect of this collection of information, including suggestions for reducing this burden, to Washington Headquarters Services, Directorate for Information Operations and Reports, 1215 Jefferson Davis Highway, Suite 1204, Arlington, VA 22202-4302, and to the Office of Management and Budget, Paperwork Reduction Project (0704-0188), Washington, DC 20503.

1. AGENCY USE ONLY (Leave blank)	2. REPORT DATE April 1996	3. REPORT TYPE AND DATES COVERED Contractor Report	
4. TITLE AND SUBTITLE NONLINEAR EXCITATION OF INVISCID STATIONARY VORTEX IN A BOUNDARY-LAYER FLOW		5. FUNDING NUMBERS C NAS1-19480 WU 505-90-52-01	
6. AUTHOR(S) Meelan Choudhari Peter W. Duck		8. PERFORMING ORGANIZATION REPORT NUMBER ICASE Report No. 96-27	
7. PERFORMING ORGANIZATION NAME(S) AND ADDRESS(ES) Institute for Computer Applications in Science and Engineering Mail Stop 132C, NASA Langley Research Center Hampton, VA 23681-0001		10. SPONSORING/MONITORING AGENCY REPORT NUMBER NASA CR-198327 ICASE Report No. 96-27	
9. SPONSORING/MONITORING AGENCY NAME(S) AND ADDRESS(ES) National Aeronautics and Space Administration Langley Research Center Hampton, VA 23681-0001		11. SUPPLEMENTARY NOTES Langley Technical Monitor: Dennis M. Bushnell Final Report To be submitted to the Journal of Fluid Mechanics.	
12a. DISTRIBUTION/AVAILABILITY STATEMENT Unclassified-Unlimited Subject Category 34		12b. DISTRIBUTION CODE	
13. ABSTRACT (Maximum 200 words) We examine the excitation of inviscid stationary crossflow instabilities near an isolated surface hump (or indentation) underneath a three-dimensional boundary layer. As the hump height (or indentation depth) is increased from zero, the receptivity process becomes nonlinear even before the stability characteristics of the boundary layer are modified to a significant extent. This behavior contrasts sharply with earlier findings on the excitation of the lower branch Tollmien-Schlichting modes and is attributed to the inviscid nature of the crossflow modes, which leads to a decoupling between the regions of receptivity and stability. As a result of this decoupling, similarity transformations exist that allow the nonlinear receptivity of a general three-dimensional boundary layer to be studied with a set of canonical solutions to the viscous sublayer equations. The parametric study suggests that the receptivity is likely to become nonlinear even before the hump height becomes large enough for flow reversal to occur in the canonical solution. We also find that the receptivity to surface humps increases more rapidly as the hump height increases than is predicted by linear theory. On the other hand, receptivity near surface indentations is generally smaller in comparison with the linear approximation. Extension of the work to crossflow receptivity in compressible boundary layers and to Görtler vortex excitation is also discussed.			
14. SUBJECT TERMS three-dimensional boundary layers; crossflow instability; receptivity; roughness			15. NUMBER OF PAGES 18
			16. PRICE CODE A03
17. SECURITY CLASSIFICATION OF REPORT Unclassified	18. SECURITY CLASSIFICATION OF THIS PAGE Unclassified	19. SECURITY CLASSIFICATION OF ABSTRACT	20. LIMITATION OF ABSTRACT

